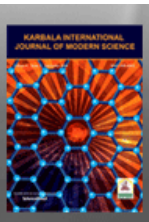
Karbala International Journal of Modern Science

Manuscript 3429

Fabrication and Characterization of Epoxy Resin Co-doped with 2,5-Diphenyloxazole and Cerium Fluoride Nanoparticles for Radiation Detection

Akapong Phunpueok

Jaruwan Seangrit

Sarawut Jaiyen

Krittiya Sreebunpeng

Wuttichai Chaiphaksa

See next page for additional authors

Follow this and additional works at: https://kijoms.uokerbala.edu.iq/home

 Part of the Biology Commons, Chemistry Commons, Computer Sciences Commons, and the Physics Commons

University of Kerbala

Fabrication and Characterization of Epoxy Resin Co-doped with 2,5-Diphenyloxazole and Cerium Fluoride Nanoparticles for Radiation Detection

Abstract

This paper presents the fabrication and characterization of a plastic scintillator prepared from epoxy resin doped with 2,5-diphenyloxazole (PPO) and cerium fluoride nanoparticles (CeF_3 NPs) for radiation detection. The CeF_3 NPs were prepared by a chemical process and examined by X-ray diffraction (XRD) and scanning electron microscopy (SEM); it was found that the prepared particles were true CeF_3 NPs with an average particle size of approximately 17 nm. The CeF_3 NPs were co-doped with PPO into epoxy resin and formed into a plastic scintillator of 3 cm in diameter and 2 cm in length. Analysis of the scintillator's luminescence properties using a fluorescence spectrometer revealed that excitation at 300 nm resulted in maximum emission at 366 nm. Scintillation response testing, conducted by coupling the plastic scintillator to a photomultiplier tube, demonstrated successful radiation detection capabilities. The optimal sample preparation conditions were determined to be 0.4% by weight of PPO doping and 0.2% by weight of CeF_3 NPs co-doping, which yielded the best gamma-ray detection performance. Energy response testing using radiation sources Na-22, Cs-137, Mn-54, and Co-60 showed that the relationship between incident gamma-ray energy and the signal measured by the multichannel analyzer exhibited 99.83% linearity. For measuring gamma rays at 662 keV, the fabricated plastic scintillator showed a light yield of 1,810 photons/MeV, corresponding to 39% of that of a commercial plastic scintillator (4,640 photons/MeV). The fabricated plastic scintillators were also responsive to X-rays and alpha particles; namely, when excited with X-rays, they exhibited a scintillation efficiency equal to 15% of that of the reference BGO crystal, and when excited with 5.5 MeV alpha particles from Pu-238, they showed an energy resolution of 48.27%.

Keywords

Cerium fluoride nanoparticles; Epoxy resin; Plastic scintillator; PPO; Radiation detection

Creative Commons License

This work is licensed under a Creative Commons Attribution-Noncommercial-No Derivative Works 4.0 License.

Authors

Akapong Phunpueok, Jaruwan Seangrit, Sarawut Jaiyen, Krittiya Sreebunpeng, Wuttichai Chaiphaksa, Kewalee Nilgumhang, and Voranuch Thongpool

RESEARCH PAPER

Fabrication and Characterization of Epoxy Resin Co-doped With 2,5-Diphenyloxazole and Cerium Fluoride Nanoparticles for Radiation Detection

Akapong Phunpueok [a], Jaruwan Seangrit [a], Sarawut Jaiyen [a], Krittiya Sreebunpeng [b], Wuttichai Chaiphaksa [c], Kewalee Nilgumhang [d], Voranuch Thongpool [a,*]

[a] Division of Physics, Faculty of Science and Technology, Rajamangala University of Technology Thanyaburi, Pathum Thani 12110, Thailand
[b] Faculty of Science, Chandrakasem Rajabhat University, Bangkok 10900, Thailand
[c] Physics Program, Faculty of Science and Technology, Nakhon Pathom Rajabhat University, Nakhon Pathom 73000, Thailand
[d] Thailand Institute of Nuclear Technology (Public Organization), Ongkharak, Nakhon Nayok 26120, Thailand

Abstract

This paper presents the fabrication and characterization of a plastic scintillator prepared from epoxy resin doped with 2,5-diphenyloxazole (PPO) and cerium fluoride nanoparticles (CeF_3 NPs) for radiation detection. The CeF_3 NPs were prepared by a chemical process and examined by X-ray diffraction (XRD) and scanning electron microscopy (SEM); it was found that the prepared particles were true CeF_3 NPs with an average particle size of approximately 17 nm. The CeF_3 NPs were co-doped with PPO into epoxy resin and formed into a plastic scintillator of 3 cm in diameter and 2 cm in length. Analysis of the scintillator's luminescence properties using a fluorescence spectrometer revealed that excitation at 300 nm resulted in maximum emission at 366 nm. Scintillation response testing, conducted by coupling the plastic scintillator to a photomultiplier tube, demonstrated successful radiation detection capabilities. The optimal sample preparation conditions were determined to be 0.4 % by weight of PPO doping and 0.2 % by weight of CeF_3 NPs co-doping, which yielded the best gamma-ray detection performance. Energy response testing using radiation sources Na-22, Cs-137, Mn-54, and Co-60 showed that the relationship between incident gamma-ray energy and the signal measured by the multichannel analyzer exhibited 99.83 % linearity. For measuring gamma rays at 662 keV, the fabricated plastic scintillator showed a light yield of 1810 photons/MeV, corresponding to 39% of that of a commercial plastic scintillator (4640 photons/MeV). The fabricated plastic scintillators were also responsive to X-rays and alpha particles; namely, when excited with X-rays, they exhibited a scintillation efficiency equal to 15% of that of the reference BGO crystal, and when excited with 5.5 MeV alpha particles from Pu-238, they showed an energy resolution of 48.27 %.

Keywords: Cerium fluoride nanoparticles, Epoxy resin, Plastic scintillator, PPO, Radiation detection

1. Introduction

A scintillator is a material that can convert ionizing radiation into visible light or UV light. Nowadays, it is applied as a radiation measuring device for various related applications, such as medical radiography, non-destructive inspection in industry, geological exploration, homeland security, space weather studies, high-energy physics research, etc. There are two main types of scintillators: inorganic scintillators and organic scintillators. Inorganic scintillators can detect high-energy radiation due to their high density, good energy resolution, and high light

Received 9 May 2025; revised 20 August 2025; accepted 23 August 2025.
Available online 23 September 2025

* Corresponding author.
E-mail address: voranut_t@rmutt.ac.th (V. Thongpool).

https://doi.org/10.33640/2405-609X.3429
2405-609X/© 2025 University of Kerbala. This is an open access article under the CC-BY-NC-ND license (http://creativecommons.org/licenses/by-nc-nd/4.0/).

output [1–5]. Many forms of inorganic scintillators exist, such as single crystals, glasses, composites, transparent ceramics, etc. The most popular form is a single crystal, found in NaI:Tl, CsI:Tl, BGO, GAGG:Ce, etc. However, their disadvantages are that they take a long time to grow, are expensive, hygroscopic, and challenging to make in large sizes. Organic scintillators, on the other hand, are characterized by fast decay times, low cost, non-hygroscopic, and easy scalability; they have the disadvantage of poor high-energy radiation detection capability due to their low density [6–10]. Many organic scintillators exist, such as single crystals, liquids, plastics, etc. The most popular form is plastic. Plastic scintillators are solids developed from different polymer bases such as polystyrene (PS), polyvinyl toluene (PVT), polyethylene naphthalate (PEN), etc. The fabrication of most plastic scintillators begins with a solution of aromatic ring monomers being heated (about 120 °C) for a long time (over 240 h) and then cooled to allow for thermal polymerization. Based on the advantages and disadvantages of inorganic and organic scintillators, a new type of composite material has been developed that can combine the benefits of both types of scintillators, namely, a new type of scintillator consisting of high-density and high-performance scintillation nanoparticles embedded in a polymer matrix that maintains the transparency of the matrix. Scientists have made new kinds of plastic scintillators by adding organometallics [11–13], nanoparticles [14–16], and lots of organic fluor to help tell the difference between pulse shapes [17–19]. During these ten years, rare earth fluoride nanoparticles have been studied intensively for various applications. The most popular rare element is cerium due to its high light output, high atomic number, and fast transition ($5d \rightarrow 4f$) of Ce^{3+}. In 2015, cerium fluoride nanoparticles (CeF_3 NPs) were synthesized chemically, mixed with polyvinyl toluene, and doped with PPO [20]. The synthesis of the plastic scintillators took more than 90 h at a temperature of 75 °C. The study found that CeF_3 NPs added to a plastic scintillator could increase the light output by 3 and 2.5 times when stimulated with UV and X-rays, respectively. This study did not report the response to other radiations, such as gamma rays, alpha particles, etc. In 2017, a plastic scintillator was produced by polymerization and tested for gamma-ray detection [21]. It was found that the scintillation light yield of synthetic plastic scintillators was approximately 50 % of that of commercial plastic scintillators and showed more than 99.7 % energy linearity. However, the study did not report the response to other radiations, such as X-rays and alpha particles, etc., and the synthesis took 250 h and uses a high temperature of 120 °C. In 2021, a PPO- and CeF_3-doped plastic scintillator was made [22]. The researchers found that CeF_3 NPs can also help increase light output. The resulting synthesized plastic scintillator could also respond to gamma radiation. Still, the measured gamma-ray spectrum differed from that of the commercial scintillator, likely because the prepared sample was thinner, making direct comparison difficult. It took 120 h to synthesize. In 2022, a PS-based scintillator doped with PPO and 1,4-bis (5-phenyl-2-oxazolyl)benzene (POPOP) was synthesized by thermal polymerization at 120 °C for over 210 h [23]. The prepared plastic scintillators were responsive to gamma and X-rays, showing a linearity of 99.85 % between the radiation energy and the received signal. Still, this study did not report the samples' scintillation light yield or compare it with commercial plastic scintillators. A PVT-based scintillator doped with PPO and POPOP was synthesized over 240 h at 120 °C in 2023 [8]. This study found that the prepared plastic scintillators responded well to gamma rays and exhibited an excellent energy linearity of 99.9 %. Still, this study did not report the response to charged radiation such as alpha particles. The preparation of plastic scintillators generally requires mixing a monomer solution with primary fluor and secondary fluor (wavelength shifters). This curing process takes several days and involves heating to over 100 °C, which is inconvenient. Therefore, epoxy resin-based plastics are another interesting alternative for preparing plastic scintillators, as they require a short preparation time (approximately 24 h), do not require high temperatures, and can be prepared at room temperature.

In the present work, we chose epoxy resin as the matrix because it has a curing time of only 24 h, can be done at room temperature, and is doped with PPO and co-doped with the synthesized CeF_3 NPs. PPO was chosen as a fluor because it has high light-emitting efficiency and a relatively low price. We studied the appropriate proportion of the components for synthesis, including testing the emission wavelength of light and the response to gamma rays, X-rays, and alpha particles. This study includes the scintillation light yields of the fabricated plastic scintillator compared with a commercial plastic scintillator in gamma-ray and alpha-particle measurements, the energy resolution for alpha particle measurement, the scintillation efficiency when excited by X-rays compared to a reference bismuth germanate (BGO) crystal, and the linear response of gamma-ray energy to the received signal.

2. Experimental

2.1. Synthesis of plastic scintillators

The preparation of cerium fluoride nanoparticles began with mixing sodium fluoride solution with cerium nitrate solution and stirring continuously at 80 °C for 4 h, then allowing it to cool to room temperature. The resulting solution was filtered, and the precipitate was washed with ethanol 3 times and dried at 50 °C for 12 h. The obtained white powder was then tested by Bruker AXS-Model D8 Advance X-ray powder diffractometer (XRD) and Hitachi US5000 FE-SEM to determine the crystal structure and microstructure. Twenty grams of the epoxy resin solution was mixed with PPO in various amounts of 0.1, 0.2, 0.3, 0.4, 0.5, 0.6, 0.7, 0.8, 0.9, and 1.0 % by weight. The solution was stirred with a magnetic stirrer for 15 min, mixed with 10 g of hardener, and stirred with a magnetic stirrer for 10 min. The resulting solution was poured into a mold and left for 24 h at room temperature. The resulting plastic blocks were obtained and tested for their emission spectra and gamma-ray responses to find the best conditions. The optimal amount of PPO was added with cerium fluoride at various amounts of 0.05, 0.10, 0.15, 0.20, 0.25, and 0.30 % by weight in epoxy resin using the same preparation method. The samples were then tested for emission spectra using a Hitachi F-4600 fluorescence spectrometer and their scintillation response using a gamma-ray spectrometer.

2.2. Scintillation response

Each plastic scintillator was connected to the Hamamatsu R6231 photomultiplier tube window using silicone grease to help with the connection. It was covered with three layers of white tape to allow the emitted light to reflect as much as possible into the photomultiplier tube (PMT). It was covered with three more layers of black tape to prevent external light from interfering. The PMT was supplied with a voltage of 800 V with a CAEN N1470B power supply. The radiation source was placed in front of the plastic scintillator. Gamma-ray photons were incident on a plastic scintillator. The plastic scintillator would change the gamma-ray photons into many visible light photons. The light photons would enter the PMT and hit the photocathode. The electrons at the photocathode would be released and accelerated to hit the next dynode, causing the electrons to be amplified and accumulated at the anode of the PMT. The resulting electrical signal would be sent to the CAEN A1424 scintillation preamplifier to cancel the noise and match the impedance. The electrical signal would enter the CAEN N6781A multichannel analyzer (MCA) to analyze the spectrum and display the results on the screen with the MC^2 program.

3. Results and discussion

3.1. X-ray diffraction (XRD)

Fig. 1 shows the crystal structure of the synthesized cerium fluoride nanoparticles. The experimental results revealed diffraction peaks at 2θ positions of 24.36°, 25.08°, 27.94°, 35.32°, 44.12°, 45.14°, 51.00°, 53.02°, 64.94°, 68.74°, and 71.38°, corresponding to the crystal planes (002), (110), (111), (112), (300), (113), (302), (211), (214), (511), and (411) of cerium fluoride. These results are consistent with JCPDS No. 08-0045 and previous reports [24]. The diffraction peaks matched the hexagonal crystal structure of CeF_3 nanoparticles. The crystallite size, calculated from the XRD spectrum using Scherrer's equation, was 16.88 nm.

3.2. Scanning electron microscopy (SEM)

Fig. 2 shows the morphology of CeF_3 NPs by scanning electron microscope at 50,000 times magnification. The image showed that CeF_3 NPs are small spherical particles. From the SEM images, the average particle size was determined using ImageJ and was found to be 16.69 ± 0.29 nm. The results from SEM aligned with those obtained from XRD, confirming that the synthesized particles are indeed in the nanoscale range.

Figs. 3 and 4 show the elemental composition spectra from the analysis using the energy-dispersive X-ray analysis technique of the synthesized

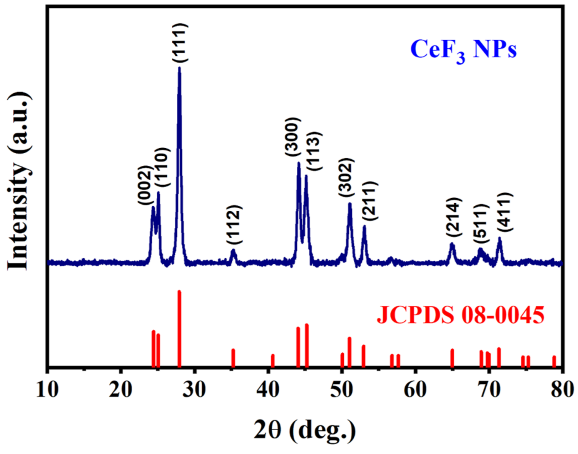

Fig. 1. X-ray diffraction pattern of CeF_3 NPs.

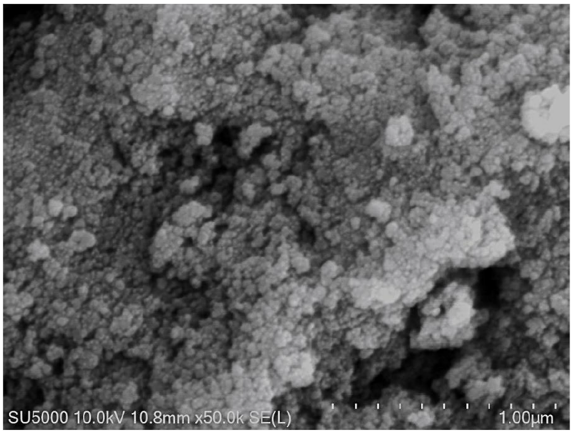

Fig. 2. Scanning electron microscope image of CeF_3 NPs.

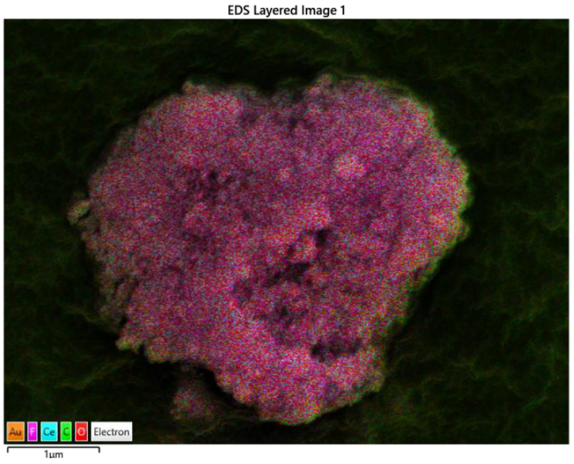

Fig. 3. Elemental composition analysis using the energy dispersive X-ray analysis technique of CeF_3 NPs.

cerium fluoride nanoparticles. From the experimental results, it was found that the CeF_3 NPs had the elemental composition of cerium (Ce) and fluorine (F) percentages by weight of 32.5 and 7.5, respectively, as shown in Table 1, which showed that the formation of CeF_3 NPs occurred.

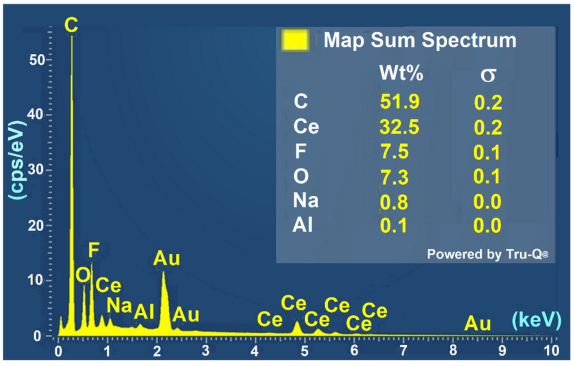

Fig. 4. Elemental composition spectra from the energy dispersive X-ray analysis technique of CeF_3 NPs.

Table 1. Elemental content of synthesized CeF_3 NPs.

Elements	Percentage by weight of each component detected (wt %)
C (Carbon)	51.9
Ce (Cerium)	32.5
F (Fluorine)	7.5
O (Oxygen)	7.3
Na (Sodium)	0.8
Al (Aluminum)	0.1

3.3. Photoluminescence (PL) and scintillation response

Fig. 5 shows the emission spectra of epoxy resins doped with different concentrations of PPO when excited with a wavelength of 300 nm. From such a figure, it was found that all spectra have the highest peak at 366 nm, and the emitted light intensity tends to rise with increasing PPO concentration. This emission wavelength is consistent with PPO-doped PVT samples reported in a previous study [22], indicating that PPO is the leading fluorescent agent despite different base polymers.

All samples were tested for gamma-ray measurement of 662 keV energy from the Cs-137 radiation source. The spectra were obtained as shown in Fig. 6. The obtained gamma-ray spectrum will not have full energy peaks; it will only be the Compton continuum. From the spectrum obtained, it will be found that the plastic with a PPO concentration of 0.4 wt % showed a spectrum with a long tail furthest to the right. This result means that epoxy resin with 0.4 wt % PPO has the best gamma-ray detection. This epoxy resin containing 0.4 wt % PPO was selected to dope with different concentrations of cerium fluoride nanoparticles, namely 0 wt %, 0.05 wt %, 0.10 wt %, 0.15 wt %, 0.20 wt %, 0.25 wt %, and 0.30 wt %.

The epoxy resin containing PPO doped with all concentrations of CeF_3 NPs was subjected to a PL

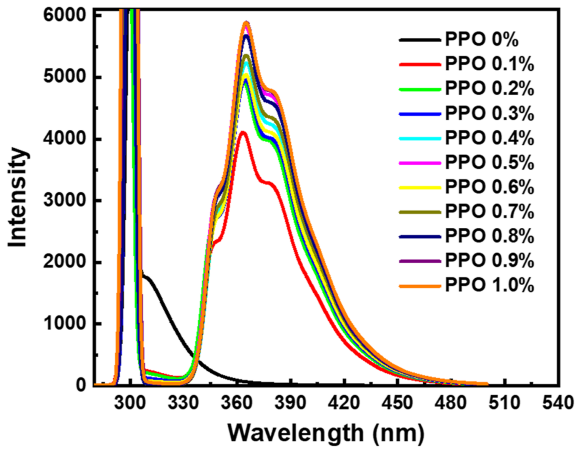

Fig. 5. Photoluminescence of fabricated PPO-doped epoxy resins.

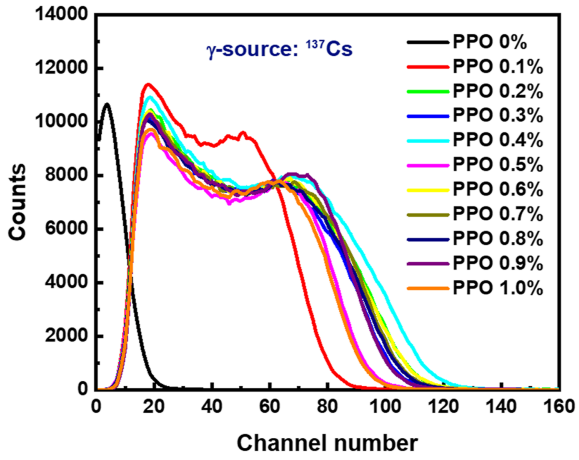

Fig. 6. Energy spectra of Cs-137 gamma source obtained from fabricated PPO-doped epoxy resins.

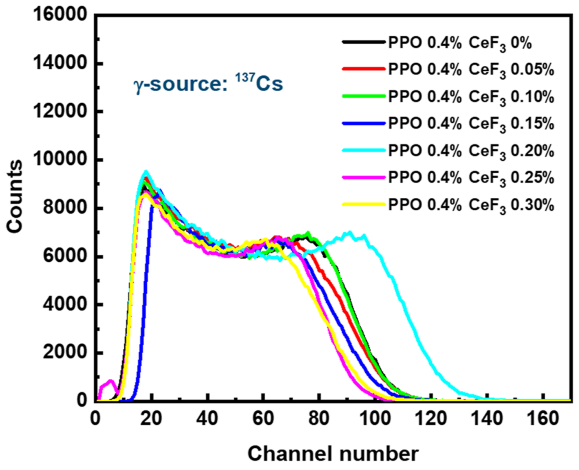

Fig. 8. Energy spectra of the Cs-137 gamma source obtained from all fabricated samples.

test, and the results are shown in Fig. 7. The figure showed that the peak intensity position remains at 366 nm in all samples because part of the excitation energy is directly excited to PPO, and part is excited to CeF_3 NPs and transferred to PPO [20]. Therefore, PPO is still the leading emitter, and the emitted light becomes more intense until the intensity decreases, indicating that the concentration of CeF_3 NPs is too high, which may cause fluorescence quenching. From the figure, it can be seen that the optimum concentration of CeF_3 NPs is 0.2 wt %. All samples were then tested for their response to gamma radiation with an energy of 662 keV from a Cs-137 source. Fig. 8 shows that the light blue line in the spectrum of the epoxy resin containing 0.4 wt % PPO and 0.2 wt % CeF_3 NPs indicates the best gamma-ray response. The best-performing sample was then compared with the BGO crystal to determine the light yield and compared with the commercial plastic scintillator of Epic Crystal Company (People's Republic of China).

The test results for measuring the spectra of 662 keV gamma rays of the three types of scintillators are shown in Fig. 9. From the figure, it can be seen that the 662 keV gamma-ray spectrum measured with the BGO crystal consists of the full energy peak and the Compton continuum, while the spectra measured with commercial and fabricated plastic scintillators do not have the full energy peak; only the Compton continuum. If observed, it will be found that the full energy peak of the BGO crystal at the left base has a separate peak, which is the X-ray escape peak of the bismuth element in the BGO crystal. It can occur when the crystal has good energy resolution and a small size, and the energy of the characteristic X-rays is very different from

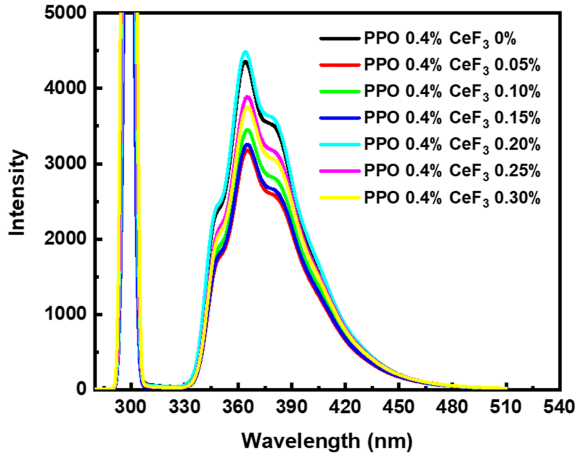

Fig. 7. Photoluminescence of fabricated epoxy resins co-doped with PPO and CeF_3 NPs.

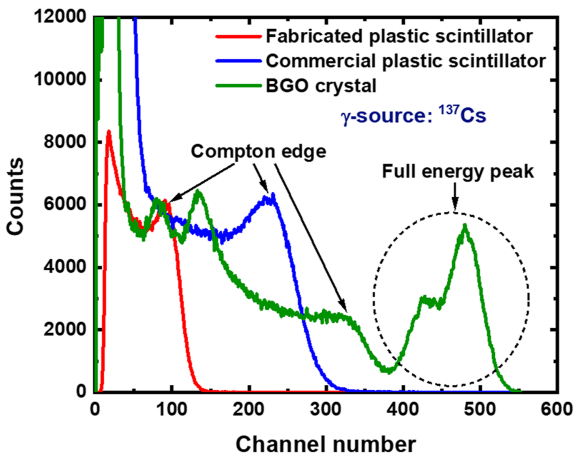

Fig. 9. Energy spectra of the Cs-137 gamma source obtained from three scintillators.

that of the full energy peak. The Compton edge is the reference point for comparison of the light emission capability of the three scintillators. From Fig. 9, it can be observed that the position of the Compton edge of the BGO crystal is furthest to the right, followed by that of the commercial plastic scintillator, and that of the fabricated plastic scintillator at the farthest to the left. This result means that the BGO crystal can emit the most significant number of photoelectrons at the photocathode, followed by the commercial plastic scintillator, and the fabricated plastic scintillator can emit the least number of photoelectrons. The number of photoelectrons in each scintillator can be determined using the Bertolaccini method [25], and the conversion of the photoelectrons into light photons emitted from the scintillator can be obtained by using the quantum efficiency (QE) of the photocathode in the photomultiplier tube (R6231 PMT). All the results are presented in Table 2.

Table 2 shows that the light yield of the BGO crystal is 4.9 times that of the fabricated plastic scintillator, and the light yield of the commercial plastic scintillator is 2.6 times that of the fabricated plastic scintillator. The light yield of 1810 photons/MeV (ph/MeV) obtained from the fabricated plastic scintillator is less than that of the plastic scintillator in a previous study [21], which is about 2850 ph/MeV. The reason may be the poor dispersion of the dopants (PPO and CeF_3 NPs). In Ref. [21], the samples were prepared using a thermal polymerization process involving prolonged heating and slow cooling, which allows for better dispersion of the dopants than epoxy resins, which cure in only 24 h at room temperature, resulting in less efficient energy transfer for scintillation. The fabricated plastic scintillator under the best conditions (0.4 wt % PPO 0.2 wt % CeF_3 NPs) was then tested for its ability to detect gamma-rays from other radiation sources, which consisted of Na-22, Mn-54, and Co-60 combined with Cs-137. The gamma-ray spectra were obtained, as shown in Fig. 10. From Fig. 10, it can be seen that the entire spectrum does not have full energy peaks, but only the Compton continuum, which can test the response of the detector by finding the relationship between the energy of the incoming radiation and the measured radiation spectrum, and whether there is a linear relationship. From Fig. 10, the position of the Compton edge was measured from the screen of the MCA, and the energy of the Compton edge is calculated from the Compton scattering equation in Equation (1).

$$E_\gamma = \frac{E_{\gamma_o}}{1 + \frac{E_{\gamma_o}}{m_o c^2}(1 - \cos\theta)} \quad (1)$$

E_{γ_o} is the energy of the full energy peak, and $m_o c^2$ is the rest mass energy of the electron, which is 511 keV. When θ is replaced by 180°, the calculated E_γ is the energy of the backscatter peak. The energy of the Compton edge peak can be found from $E_{\gamma_o} - E_\gamma$, which was shown in Table 3. When the Compton edge energy in Table 3 is plotted against the Compton edge position on the screen of the MCA in Fig. 10, four points are obtained. A straight-line graph called the energy calibration curve of the scintillation detector is shown in Fig. 11. When the

Table 2. Light yield and photoelectron yield at 662 keV gamma-ray energy of three scintillators.

	BGO crystal	Commercial plastic scintillator	Fabricated plastic scintillator
Channel number of the Compton edge	333	226	91
Photoelectron yield (phe/MeV)	2205	1497	603
Maximum wavelength (nm)	480	415	366
Quantum efficiency (%)	24.64	32.28	33.32
Light yield (ph/MeV)	8950	4640	1810

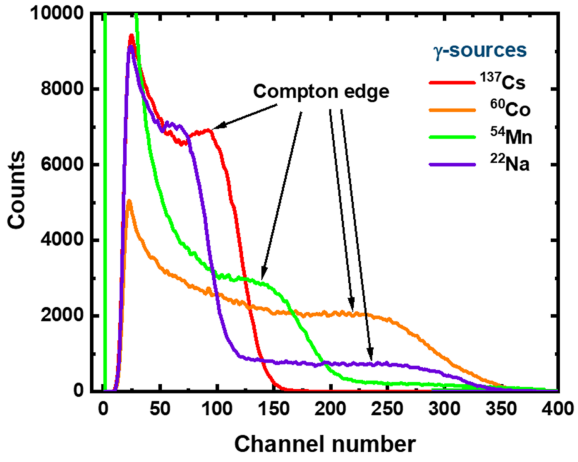

Fig. 10. Gamma-ray spectra obtained from the fabricated plastic scintillator.

Table 3. Compton edge energies are calculated from four types of gamma-ray sources.

Gamma source	Gamma-ray energy (keV)	Compton edge energy (keV)
Cs-137 (^{137}Cs)	662	477
Mn-54 (^{54}Mn)	835	639
Co-60 (^{60}Co)	1173/1333	1041 (avg.)
Na-22 (^{22}Na)	1275	1062

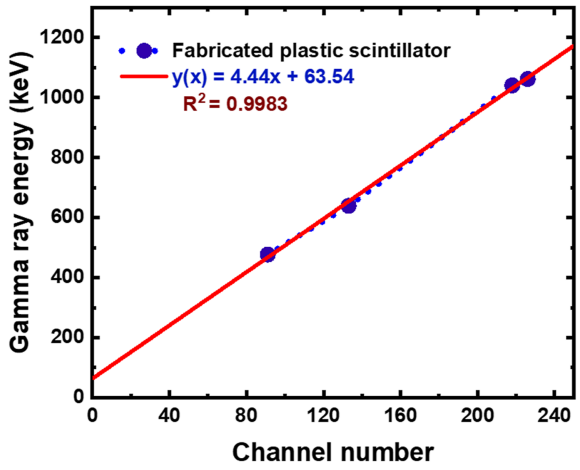

Fig. 11. Energy calibration curve obtained from the fabricated plastic scintillator prepared from epoxy resin doped with 0.4 wt % PPO and 0.2 wt % CeF_3 NPs.

linearity is calculated, it was found that the R^2 value is 0.9983 or 99.83 %, which is considered quite linear. This result indicates that if this fabricated plastic scintillator is used as a radiation detector, it can respond very well to different radiation energies. The linearity value obtained in this work (99.83 %) is comparable to those reported in previous studies—99.7 % and 99.85 %, respectively [21,23].

Fig. 12 shows the radioluminescence (RL) spectra of the BGO crystal and the fabricated plastic scintillator measured at room temperature under the same experimental conditions. The fabricated plastic scintillator showed an RL emission band with an integral scintillation efficiency of about 15 % of the reference BGO crystal. This result aligned with the gamma-ray excited light yield results in Fig. 9 and the light yield values in Table 2. This result demonstrated that the fabricated plastic scintillator is less responsive to high-energy photons than a BGO crystal. These results indicate that the charge transport efficiency in the scintillation mechanism of the BGO crystal is significantly superior to that of the fabricated plastic scintillator.

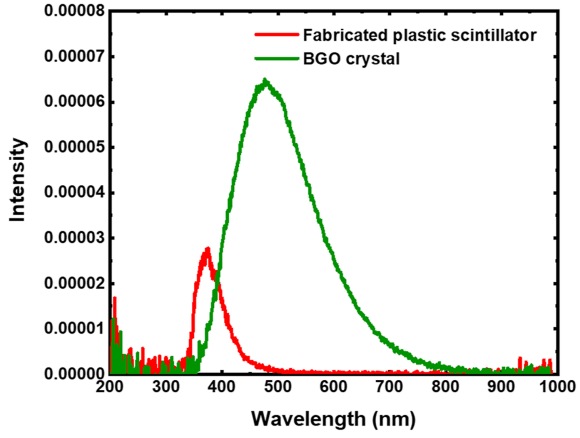

Fig. 12. X-ray-excited luminescence (XEL) spectra of the fabricated plastic scintillator and BGO crystal.

Energy spectra of 5.5 MeV alpha particles obtained from the fabricated plastic and the commercial plastic scintillators at room temperature are shown in Fig. 13. The photoelectron yield, light yield, and energy resolution at a 5.5 MeV alpha source are displayed in Table 4. The photoelectron yield in the phe/MeV unit of alpha particles was determined using the Bertolaccini method by relating the position of a photopeak of alpha particles detected in both samples with that of a single photoelectron peak from a photocathode in the photomultiplier tube. The LY (ph/MeV) was recalculated from the photoelectron yield in photoelectrons/MeV unit (phe/MeV), assuming the R6231 PMT quantum efficiency of 32.28 % for peak emission (415 nm) of the commercial plastic scintillator and that of 33.32 % for peak emission (366 nm) of the fabricated plastic scintillator. From Table 4, it can be seen that the light yield of the commercial plastic scintillator is 5.8 times that of the fabricated plastic scintillator. The energy resolution of the full

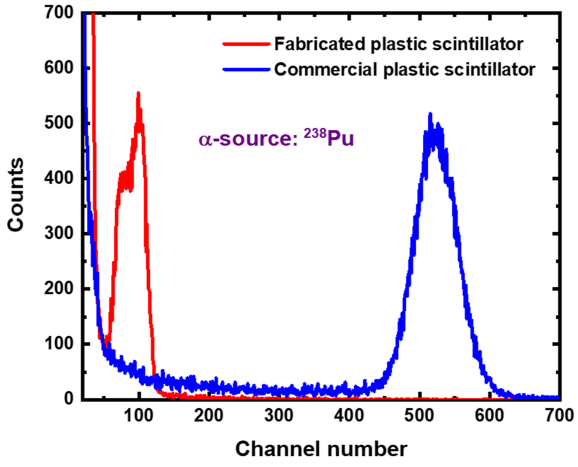

Fig. 13. Energy spectra of 5.5 MeV alpha particles were obtained from fabricated plastic and commercial plastic scintillators.

Table 4. Photoelectron yield, light yield, and energy resolution at 5.5 MeV alpha particle energy from Pu-238 of both scintillators.

	Commercial plastic scintillator	Fabricated plastic scintillator
Photoelectron yield (phe/MeV)	124	22
Light yield (ph/MeV)	384	66
Energy resolution (%)	13.71	48.27

energy peak obtained from the commercial plastic scintillator is 13.71 %, better than the 48.27 % obtained from the fabricated plastic scintillator. This result is probably due to the fabricated plastic scintillator's poor light yield. The energy resolution is strongly correlated with the light yield of the scintillation material [26,27]. The 48.27 % energy resolution observed in this study is slightly worse than the 46.22 % reported in a previous study [28], in which a plastic scintillator was prepared from epoxy resin doped with 2-(4-biphenylyl)-5-(4-tert-butylphenyl)-1,3,4-oxadiazole (b-PBD) and 1,4-bis (2-methylstyryl)benzene (Bis-MSB). That study measured 5.49 MeV alpha particles from an Am-241 source. The difference in performance is likely due to the sample thickness: their scintillator was only 1 mm thick, whereas the sample in this work was 20 mm thick. Reduced thickness allows more scintillation photons to escape (minimizing light reabsorption), thereby increasing light yield and improving energy resolution.

4. Conclusion

The synthesized cerium fluoride nanoparticles, characterized by SEM and XRD, exhibited nanoscale particle sizes of approximately 17 nm. The fabricated plastic scintillator could be prepared within 24 h at room temperature. Under UV excitation, it showed a maximum emission wavelength of 366 nm. The optimal preparation conditions were 0.4 wt % PPO and 0.2 wt % CeF_3 nanoparticles. The light yield at 662 keV gamma-ray energy was 1810 ph/MeV, with a linear correlation of 99.83 % between the gamma-ray energy and the measured signal. The X-ray–excited scintillation efficiency was 15 % of that of the reference BGO crystal. The energy resolution at 5.5 MeV from a ^{238}Pu α-source was 48.27 %. The fabricated scintillator could detect gamma rays, X-rays, and alpha particles, producing spectra for gamma rays and alpha particles similar to those of a commercial plastic scintillator. Its main advantages included rapid preparation, lower cost than imported plastic scintillators, and no requirement for high-temperature processing. However, the light yield under radiation excitation remained relatively low. Future improvements should focus on incorporating additional dopants to enhance light emission efficiency and developing techniques to achieve better dopant dispersion.

Ethics information

This study did not involve the use of animal or human subjects.

Funding

This research was supported by the Science, Research and Innovation Promotion Funding (TSRI) (Grant no. FRB660012/0168). This research block grants were managed under Rajamangala University of Technology Thanyaburi (FRB66E0623).

Conflicts of interest

The authors declare that they have no known competing financial interests or personal relationships that could have appeared to influence the work reported in this paper.

Acknowledgements

The authors would like to thank the Science, Research and Innovation Promotion Funding (TSRI) (Grant no. FRB660012/0168). This research block grants were managed under Rajamangala University of Technology Thanyaburi (FRB66E0623).

References

[1] M. Moszynski, Inorganic scintillation detectors in γ-ray spectrometry, Nucl. Instrum. Methods Phys. Res. A 505 (1–2) (2003) 101–110, https://doi.org/10.1016/S0168-9002(03)01030-1.
[2] C.L. Melcher, Perspectives on the future development of new scintillators, Nucl. Instrum. Methods Phys. Res. A 537 (1–2) (2005) 6–14, https://doi.org/10.1016/j.nima.2004.07.222.
[3] M. Nikl, Scintillation detectors for x-rays, Meas. Sci. Technol. 17 (4) (2006) R37–R54, https://doi.org/10.1088/0957-0233/17/4/R01.
[4] D. Zhu, M. Nikl, W. Chewpraditkul, J. Li, Development and prospects of garnet ceramic scintillators: a review, J Adv Ceram 11 (12) (2022) 1825–1848, https://doi.org/10.1007/s40145-022-0660-9.
[5] K. Sreebunpeng, W.R. Chewpraditkul, N. Pattanaboonmee, W. Chewpraditkul, R. Kucerkova, V. Babin, Y. Wang, D. Zhu, C. Hu, M. Nikl, J. Li, Temperature-dependent characteristics, light yield nonproportionality, and intrinsic energy resolution of Ce,Mg:$Lu_2Y(Al,Ga)_5O_{12}$ garnet ceramics, Radiat. Phys. Chem. 236 (112886) (2025) 1–6, https://doi.org/10.1016/j.radphyschem.2025.112886.
[6] S.W. Moser, W.F. Harder, C.R. Hurlbut, M.R. Kusner, Principles and practice of plastic scintillator design, Radiat. Phys. Chem. 41 (1–2) (1993) 31–36, https://doi.org/10.1016/0969-806X(93)90039-W.
[7] E. Montbarbon, Z. Zhang, A. Grabowski, R. Woo, D. Tromson, C. Dehé-Pittance, R.B. Pansu, G.H.V. Bertrand, M. Hamel, The role of the secondary fluorophore in ternary plastic scintillators aiming at discriminating fast neutrons from gamma-rays, J Lumin 213 (September) (2019) 67–74, https://doi.org/10.1016/j.jlumin.2019.04.059.
[8] L. Alex, R. Paulraj, Sonu, M. Tyagi, Development of large size fast timing and radiation resistant PVT-based plastic scintillator detector, J Mater Sci Mater Electron 34 (127) (2023) 1–12, https://doi.org/10.1007/s10854-022-09577-9.
[9] M. Koshimizu, Fundamental processes and recent development of organic scintillators, J Lumin 278 (121008) (2025) 1–14, https://doi.org/10.1016/j.jlumin.2024.121008.

[10] D.A. Kumar, E. Parthiban, Recent advancements of organic scintillators in enhancing the performance of fast neutron detection: a review, Nucl. Anal. 4 (100171) (2025) 1–6, https://doi.org/10.1016/j.nucana.2025.100171.
[11] M. Koshimizu, G.H.V. Bertrand, M. Hamel, S. Kishimoto, R. Haruki, F. Nishikido, T. Yanagida, Y. Fujimoto, K. Asai, X-ray detection capability of bismuth-loaded plastic scintillators, Jpn J Appl Phys 54 (102202) (2015) 1–5, https://doi.org/10.7567/JJAP.54.102202.
[12] H.A. Yemam, A. Mahl, U. Koldemir, T. Remedes, S. Parkin, U. Greife, A. Sellinger, Boron-rich benzene and pyrene derivatives for the detection of thermal neutrons, Sci Rep 5 (13401) (2015) 1–9, https://doi.org/10.1038/srep13401.
[13] I.B. Nemchenok, N.A. Gundorin, E.A. Shevchik, A. A. Shurenkova, Plastic scintillators for thermal neutrons detection, Funct. Mater. 20 (3) (2013) 310–314, https://doi.org/10.15407/fm20.03.310.
[14] A. Magi, M. Koshimizu, A. Watanabe, A. Yoko, G. Seong, T. Tomai, T. Adschiri, R. Haruki, F. Nishikido, S. Kishimoto, Y. Fujimoto, K. Asai, Optimization of phosphor concentration of surface-modified Bi_2O_3 nanoparticle-loaded plastic scintillators for high-energy photon detection, J Mater Sci Mater Electron 32 (March) (2021) 7987–7999, https://doi.org/10.1007/s10854-021-05522-4.
[15] C. Frangville, A. Grabowski, J. Dumazert, E. Montbarbon, C. Lynde, R. Coulon, A. Venerosy, G.H.V. Bertrand, M. Hamel, $^{6}Li_2^{10}B_4O_7$ NPs-loaded plastic scintillators for fast/thermal neutron and gamma ray detection, Mater Chem Front 3 (8) (2019) 1574–1579, https://doi.org/10.1039/C9QM00222G.
[16] H. Tsukahara, M. Koshimizu, Development of $LiGaO_2$ nanoparticle-loaded plastic scintillators for thermal neutron detection, J Mater Sci Mater Electron 36 (1223) (2025) 1–11, https://doi.org/10.1007/s10854-025-15288-8.
[17] N.P. Zaitseva, A.M. Glenn, A.N. Mabe, M.L. Carman, C. R. Hurlbut, J.W. Inman, S.A. Payne, Recent developments in plastic scintillators with pulse shape discrimination, Nucl. Instrum. Methods Phys. Res. A 889 (May) (2018) 97–104, https://doi.org/10.1016/j.nima.2018.01.093.
[18] N. Zaitseva, A. Glenn, H.P. Martinez, L. Carman, I. Pawełczak, M. Faust, S. Payne, Pulse shape discrimination with lithium-containing organic scintillators, Nucl. Instrum. Methods Phys. Res. A 729 (November) (2013) 747–754, https://doi.org/10.1016/j.nima.2013.08.048.
[19] I.A. Pawełczak, A.M. Glenn, H.P. Martinez, M.L. Carman, N. P. Zaitseva, S.A. Payne, Boron-loaded plastic scintillator with neutron-γ pulse shape discrimination capability, Nucl. Instrum. Methods Phys. Res. A 751 (July) (2014) 62–69, https://doi.org/10.1016/j.nima.2014.03.027.
[20] S. Sahi, W. Chen, K. Jiang, Luminescence enhancement of PPO/PVT scintillators by CeF_3 nanoparticles, J Lumin 159 (March) (2015) 105–109, https://doi.org/10.1016/j.jlumin.2014.11.004.
[21] C.H. Lee, J. Son, T.H. Kim, Y.K. Kim, Characteristics of plastic scintillators fabricated by a polymerization reaction, Nucl. Eng. Technol. 49 (3) (2017) 592–597, https://doi.org/10.1016/j.net.2016.10.001.
[22] V. Thongpool, A. Phunpueok, S. Jaiyen, N. Choosakul, D. Aphairaj, P. Thongchai, C. Singhaseree, Preparation of CeF_3 nanoparticles loaded PPO/PVT composites for radiation detection, Dig. J. Nanomater. Bios. 16 (2) (2021) 621–625, https://doi.org/10.15251/DJNB.2021.162.621.
[23] L. Alex, R. Paulraj, M. Tyagi, Effect of PPO and POPOP activators on the scintillation performance of polystyrene-based scintillator, J. Optoelectron. Adv. Mater. 24 (7–8) (2022) 365–371. https://joam.inoe.ro/articles/effect-of-ppo-and-popop-activators-on-the-scintillation-performance-of-polystyrene-based-scintillator/.
[24] Y. Li, Y. Cai, C. Ming, H. Chen, J. Zhang, A. Zhou, F. Song, F. Yuan, Y. Qin, G. Zhang, Q. Wang, Z. Zhao, Simple synthesis, adjusting luminescence colour and white light emission of Ln^{3+}: CeF_3 (Ln = Tm, Tb, Eu) phosphors, Bull. Mater. Sci. 46 (113) (2023) 1–8, https://doi.org/10.1007/s12034-023-02955-x.
[25] M. Bertolaccini, S. Cova, C. Bussolatti, A technique for absolute measurement of the effective photoelectron per keV yield in scintillation counters, in: International Symposium on Nuclear Electronics, 1968, pp. 1–8. Versailles, France.
[26] M. Moszynski, J. Zalipska, M. Balcerzyk, M. Kapusta, W. Mengesha, J.D. Valentine, Intrinsic energy resolution of NaI(Tl), Nucl. Instrum. Methods Phys. Res. A 484 (1–3) (2002) 259–269, https://doi.org/10.1016/S0168-9002(01)01964-7.
[27] P. Dorenbos, J.T.M. de Haas, C.W.E. van Eijk, Non-proportionality in the scintillation response and the energy resolution obtainable with scintillation crystals, IEEE Trans Nucl Sci 42 (6) (1995) 2190–2202, https://doi.org/10.1109/23.489415.
[28] R.M. Sahani, A. Pandya, Novel epoxy-bPBD-BisMSB composite plastic scintillator for alpha, beta and gamma radiation detection, Sci Rep 14 (6531) (2024) 1–10, https://doi.org/10.1038/s41598-023-45501-9.